Submitted to the 7th International Conference on Computer Vision

# Multiscale Statistical Image Invariants

Terry S. Yoo

National Library of Medicine,
The National Institutes of Health, 8600 Rockville Pike, Bethesda, MD 20894, USA

**Abstract**

It is often necessary to evaluate measured features of an image with respect to estimated properties of noise incorporated with the image values. In some cases, differential geometric methods lead to erroneous decisions arising from the assumption of linearity of the noisy feature space. This paper introduces new work in multiscale image statistics, a local framework that supports adaptive measurement of image structure with unknown and often non-stationary noise functions. Furthermore, it presents directional local statistics that enable the local normalization of feature measurement, reducing biases in noise measurement introduced by the underlying image geometry. Such measurements have applications in nonlinear filtering, texture analysis, and image segmentation.

## 1. Introduction and Background

When digital images are considered as arrays of observations made of an underlying scene, the vocabulary and calculus of statistics may be applied to their analysis. If an image is subject to noise in pixel measurement, it should be presented within the context of either known or computed properties of the pixel values. These properties include the sample size or raster resolution and other statistics such as the variance of the additive noise.

This is an introduction to multiscale image statistics. It presents central moments of the local probability distribution of intensity values. It assumes that images are composed of piecewise ergodic regions (that is, piecewise contiguous regions where spatial averaging may be traded for repeated measurement) for the construction of multiscale statistics. This approach outlines the generation of the central moments of the local intensity histogram of any arbitrary order. Properties of some of these moments are explained, their behaviors are compared with other image processing operators, and the multiscale central moments are generalized to images of two dimensions. Directional versions of these multiscale statistics are also developed, and their future uses in the normalization of feature measurements are discussed.

### 1.1. Statistical Analysis

Statistical pattern recognition is a discipline with a long and well-established history. Segmentation and filtering strategies based on local and global neighborhood statistics are well documented (e.g., Duda [6] or Jain [13]). Filters founded on the theory of Markov processes (Markov Random Fields) [11, 2] as well as expectation-maximization methods [5] also have a long history. Geiger and Yuille provide a framework for comparing these and other segmentation strategies in their survey of a variety of different algorithms [10].

Typically, statistical methods in image processing employ the distribution of intensities computed at the maximum outer scale of the image. That is, the histograms, mixture models, or probability distribution approximations are computed across the whole image, including all pixel values equally. Exceptions to this generalization include the contrast enhancement methods for adaptive histogram equalization (AHE). AHE and its derivatives (Contrast limited AHE (CLAHE), and Sharpened AHE or (SHAHE)) construct local histograms of image intensity and compute new image values that generate an equalized local probability distribution. [21, 3]. Other exceptions include Markov random fields [11] and sigma filters [17]. Questions often arise over the priors used in sigma filters and smoothing based on Markov random fields. Other questions arise over the selection of the neighborhood function.

### 1.2. Directional Analysis

Local directional image analysis techniques (including the Kirsch, Sobel, and Gabor filters) are described in most introductory texts on image processing (e.g., [13]). Of greater interest is the more recent development of scale-space representations along with their differential invariants. Notably, researchers such as Koenderink [14,16], ter Haar Romeny [22,23], Florack [8,9], Lindeberg [18,19], and Eberly [7] have contributed many papers on scale space and the invariances of scale-space derivatives. Perona noted that directional derivatives of arbitrary order can be constructed through

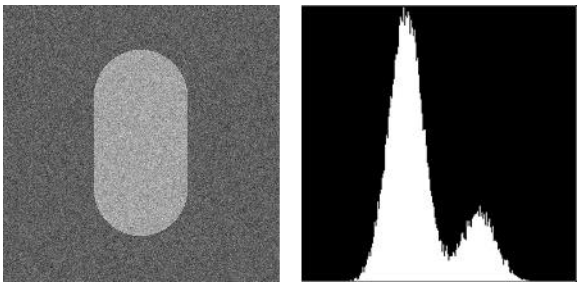

Figure 1. Test figure with global histogram. Left: Test figure is 256 × 256 with a background pixel intensity of 0 and a foreground value of 64. Additive uncorrelated noise has variance of 256. Right: the global histogram shows the asymmetric bimodal distribution of pixel intensities

linear combinations of scale-space derivatives [20]. However, this steerable property is not limited to the Gaussian as a filter function and holds for any kernel whose n-th order derivative exists [19].

The Hessian and other matrix forms have been used extensively in the analysis of the height fields of images and other 2-manifolds representing solid shape. Koenderink describes the detection of principal curvature directions and the subsequent extraction of ridges of 2-manifolds in 3-space [15]. Gueziec and Ayache extract ridges of principal curvature as aids in registration of 3D datasets [12]. In 2D, Whitaker uses the Hessian in his nonlinear analysis to find medial axes [26]. Similarly, Lindeberg uses the *windowed second-moment matrix*, a linear algebraic operator in the analysis of image texture [18]. Weickert applies this operator in nonlinear filtering of highly figured data [24].

The approaches described above are not easily made invariant with respect to linear functions of image intensity, nor are they easily generalized to multivalued functions when the individual values cannot be considered a vector value. What is desired is a method that is invariant to transformations such as changes in contrast or gain and shifts of the background or baseline intensity. In this research, multiscale directional means and directional variances of intensity are derived from their basic definitions. Singular value decomposition of the resulting directional covariance matrix produces eigenvalues and eigenvectors that reflect image structure. These eigenvalues have the desired invariances with respect to rotation, translation, and linear functions of intensity. The work presented in this paper diverges from the more common study of the local differential structure of images. It investigates the use of statistics of local intensity distributions to illuminate image structure.

### 1.3. Local Statistics of Image Intensity

As with most statistical pattern recognition systems, this research is based on the assumption that the input

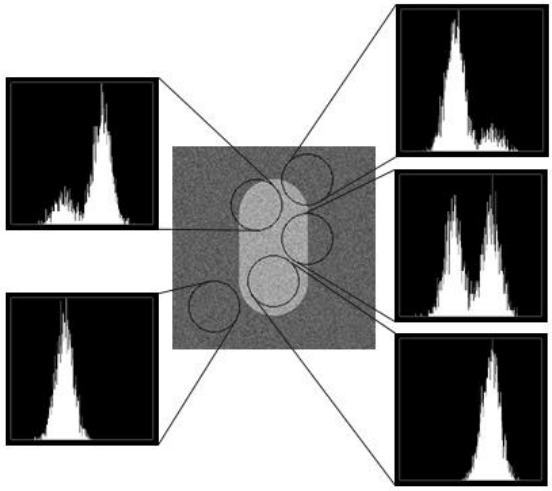

Figure 2. Test figure with local histograms. Histograms of pixel intensities shown for the local regions depicted by the gray circles. Note the changing symmetry of the local histograms depending on the overlap of the neighborhood, the figure, and the background.

signal follows a Gibbs distribution. Stated loosely, this implies that the value for the intensity at a particular location has compact local support. Under these conditions, it is expected that a scaled derivative measurement at a particular location or pixel is supported by the local neighborhood of surrounding pixels. Similarly, in the context of local statistics of image patterns, a statistical measurement is expected to be consistent over a local neighborhood. Modest changes in the size and the location of the measurement region should induce smooth changes in the extracted statistics.

Consider the lozenge shaped object in Figure 1. The foreground pixel intensity has a mean brightness of 64 units, and the background has a mean of 0 units. The image has uncorrelated Gaussian distributed additive "white" noise, zero-mean with a standard deviation of 16 units. The image is 256 × 256 pixels. If one considers the entire distribution of brightness levels throughout the image, the result is the histogram on the right side of Figure 1. Notice the asymmetry of the distribution. The global nature of the histogram limits the conclusions drawn from generalizations of the entire image.

However, if distributions of local neighborhoods within the image are considered, more specific conclusions can be drawn, and conjectures can be made that accurately describe the geometry of the image. Consider the same image with histograms extracted not from the whole image, but from individual regions. Figure 2 shows five histograms of five local regions from the image. When the local region is taken from only the foreground or only from the background intensities, a simple distribution with a single mode arises. When the local neighborhood is evenly balanced between object and

background, a symmetric bimodal distribution is generated. Finally, when the number of foreground and background pixels is not evenly balanced, a skewed distribution results, with the skew favoring the pixel values that appear in greater number.

As the sample neighborhood smoothly varies its location, certain patterns arise. For example, a local region with a balanced bimodal distribution of intensities suggests a boundary between two regions. As the location of the local sampling region is perturbed, nearby locations where similar conditions of balanced bimodal intensity distributions are exposed. Following the set of all connected loci where this condition is met will extrude a perimeter where boundariness can be evaluated. Moreover, the histograms themselves suggest a means of determining the strength of that boundary, even relative to the noise in the image. The separation between the two modes can be captured and evaluated relative to the spread or dispersion of intensity values about the modes.

While the combined set of local histograms can be illuminating, it is both inconvenient and unwieldy to generate and analyze a local histogram for each pixel in the image. A more compact description of the distribution of local image intensities is desired. One means of describing any distribution of samples is through the generation of its central moments, a series of descriptive statistics of the sample set. In the case of image analysis, *multiscale image statistics* not only capture the local intensity distribution, they can also be calculated directly from the image without the intermediate step of first generating local histograms.

## 2. Multiscale Statistics

Without *a priori* knowledge of the boundaries and the object widths within an image, locally adaptive multiscale statistical measurements are required to analyze the probability distribution across an arbitrary region of an image. This section presents multiscale image statistics, a technique developed through this research for estimating central moments of the probability distribution of intensities at arbitrary locations within an image across a continuously varying range of scales. Related work on the first order absolute moment has been presented previously by Demi [4]. My research is not a continuation, but rather a separate formal presentation of the general form of multiscale image statistics.

Consider a set of observed values, $\bar{I}(x) \subset R^1$, where for purposes of discussion the location $x \in R^1$, but can easily be generalized to $R^n$. The values of $\bar{I}(x)$ may be sampled over a local neighborhood about a particular location x using a weighting function, $\omega(x)$, and the convolution operation, $\bar{I}(x) \otimes \omega(x)$, where

$$\bar{I}(x) \otimes \omega(x) = \int_{-\infty}^{\infty} \omega(\tau)\bar{I}(x-\tau)d\tau = \int_{-\infty}^{\infty} \omega(x-\tau)\bar{I}(\tau)d\tau \quad (1)$$

To avoid a preference in orientation or location, the sampling function should be invariant with respect to spatial translation and spatial rotation. Arguments put forward by Babaud [1], Koenderink [14], ter Haar Romeny [11], Florack [9], Witkin [27], and others suggest that the optimal sampling function is the Gaussian $G(\sigma,x)$, where the parameter $\sigma$ is the sampling aperture.

$$\omega(x) = G(\sigma, x) = \frac{1}{\sigma\sqrt{2\pi}} e^{-\frac{x^2}{2\sigma^2}} \quad (2)$$

Throughout this section, multiscale statistics will be graphically illustrated using a step edge with additive noise as an input function (see Figure 3).

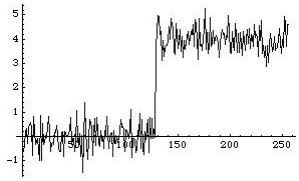


Figure 3. An example input Signal $\bar{I}(x)$ - a noisy 1D step.

### 2.1. Multiscale Mean

Let the scale-space measurement comprised of a sum of the original image intensities weighted by a Gaussian sampling kernel be the average or expected value of $\bar{I}(x)$ over the neighborhood with an aperture of size $\sigma$. Thus:

$$\begin{aligned} \mu_{\bar{I}}(x \mid \sigma) &= \left\langle \bar{I}(x); \sigma \right\rangle = \int_{-\infty}^{\infty} G(\sigma, x-\tau)\bar{I}(\tau)d\tau \\ &= \bar{I}(x) \otimes G(\sigma, x) \end{aligned} \quad (3)$$

where $\langle \bar{I}(x);\sigma \rangle$ is read as mean or the expected value of $\bar{I}(x)$ measured with aperture $\sigma$.

Figure 4 shows the multiscale mean operator applied at four different scales. As with all scale-space operators, one must balance noise suppression and precision.

### 2.2. Multiscale Variance

The local variance over the neighborhood specified by the scale parameter is easily generalized from the basic definition of central moments. Equation (4) describes the local variance of intensity about a point x at scale $\sigma$.

$$\begin{aligned} \mu_{\bar{I}}^{(2)}(x \mid \sigma) &= \left\langle \left(\bar{I}(x) - \mu_{\bar{I}}(x \mid \sigma)\right)^2; \sigma \right\rangle \\ &= \int_{-\infty}^{\infty} G(\sigma, x-\tau)\left(\bar{I}(\tau) - \mu_{\bar{I}}(x \mid \sigma)\right)^2 d\tau \\ &= G(\sigma, x) \otimes \left(\bar{I}(x)\right)^2 - \left(\mu_{\bar{I}}(x \mid \sigma)\right)^2 \end{aligned} \quad (4)$$

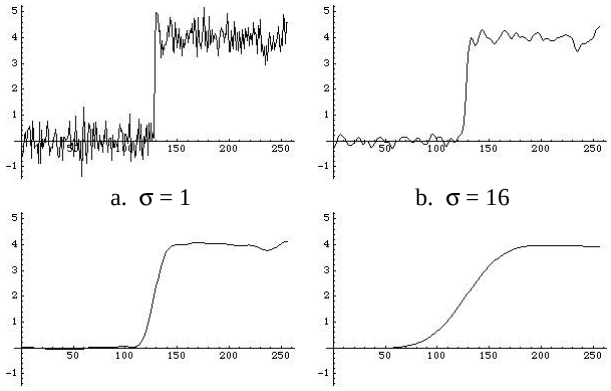

a. $\sigma = 1$ b. $\sigma = 16$ c. $\sigma = 24$ d. $\sigma = 32$

Figure 4. 1D multiscale mean operator $\mu_{\bar{I}}(x|\sigma)$ for the input function shown in Fig. 3. Four different apertures are applied (a. $\sigma = 1$, b. $\sigma = 16$, c. $\sigma = 24$, d. $\sigma = 32$).

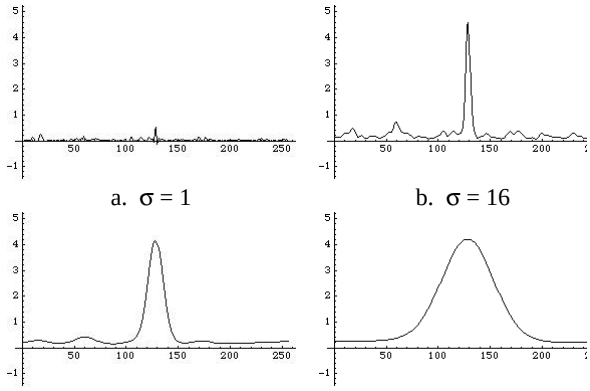

a. $\sigma = 1$ b. $\sigma = 16$ c. $\sigma = 24$ d. $\sigma = 32$

Figure 5. $\mu_{\bar{I}}^{(2)}(x \mid \sigma)$, 1D multiscale variance operator for the function in Fig. 3. Four different apertures are applied. (a. $\sigma = 1$, b. $\sigma = 16$, c. $\sigma = 24$, d. $\sigma = 32$).

Figure 5 shows the multiscale variance operator applied at four different scales. Note that the maximum of the variance function localizes about the discontinuity and remains in the same location as scale changes. This behavior is similar to the gradient magnitude operator. Both are invariant with respect to rotation and translation, and both have similar responses to a given input stimulus.

### 2.3. Other Multiscale Central Moments

The general form for the multiscale central moment of order k of $\bar{I}(x)$ is given by

$$\begin{aligned}\mu_{\bar{I}}^{(k)}(x \mid \sigma) &= \left\langle \left(\bar{I}(x) - \mu_{\bar{I}}(x \mid \sigma)\right)^k ; \sigma \right\rangle \\ &= G(\sigma, x) \otimes \left(\bar{I}(x) - \mu_{\bar{I}}(x \mid \sigma)\right)^2 \\ &= \int_{-\infty}^{\infty} G(\sigma, x - \tau)\left(\bar{I}(\tau) - \mu_{\bar{I}}(x \mid \sigma)\right)^k d\tau\end{aligned} \tag{5}$$

Figures 6 and 7 show the multiscale responses of the 3rd and 4th order central moments of the function from Figure 3 respectively. The 3rd order central moment (reflecting skew) has a zero crossing at the locus of the discontinuity that persists through changes in scale. Similarly, the 4th order moment has a local minimum at the discontinuity which also persists through scale.

### 2.4. Multiscale Statistics of 2D Images

Extending the construction of multiscale statistics to images of two dimensions is straightforward. The central moments are constrained to be invariant with respect to rotation as well as translation. These constraints specify an isotropic Gaussian as the sampling kernel. The general form for the k-th multiscale central moment for 2D images is

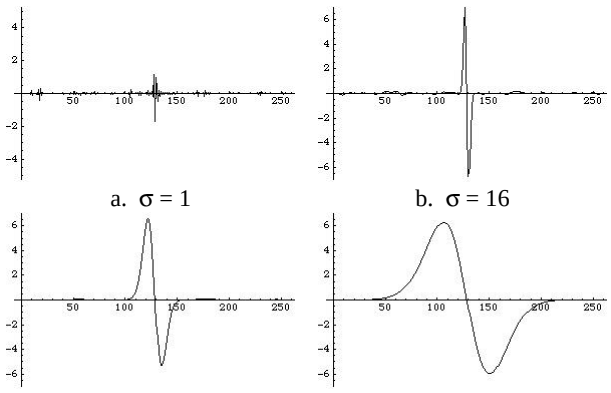

a. $\sigma = 1$ b. $\sigma = 16$ c. $\sigma = 24$ d. $\sigma = 32$

Figure 6. $\mu_{\bar{I}}^{(3)}(x \mid \sigma)$ 1D multiscale 3rd order central moment operator with four apertures for the function in Fig. 3. (a. $\sigma = 1$, b. $\sigma = 16$, c. $\sigma = 24$, d. $\sigma = 32$).

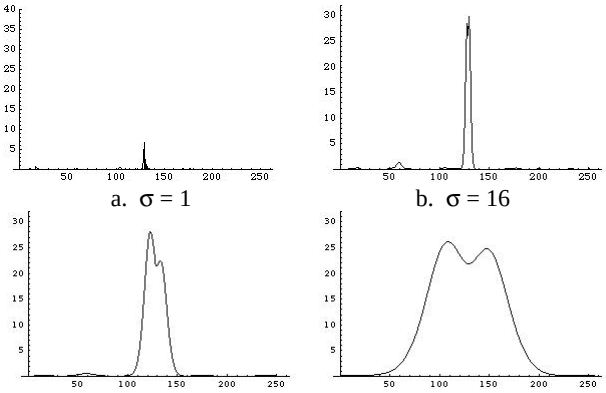

a. $\sigma = 1$ b. $\sigma = 16$ c. $\sigma = 24$ d. $\sigma = 32$

Figure 7. $\mu_{\bar{I}}^{(4)}(x \mid \sigma)$, 4th order central moment operator applied to the function from Fig. 3. (a. $\sigma = 1$, b. $\sigma = 16$, c. $\sigma = 24$,d. $\sigma = 32$).

$$\mu_{\bar{I}}^{(k)}(\mathbf{p}\mid\sigma)=\left\langle\left(\bar{I}(\mathbf{p})-\mu_{\bar{I}}(\mathbf{p}\mid\sigma)\right)^{k};\sigma\right\rangle$$
$$=G(\sigma,\mathbf{p})\otimes\left(\bar{I}(\mathbf{p})-\mu_{\bar{I}}(\mathbf{p}\mid\sigma)\right)^{k} \quad (6)$$
$$=\frac{1}{\sigma^2 2\pi}\int_{-\infty}^{\infty}\int_{-\infty}^{\infty}e^{\frac{-((p_X-\tau)^2+(pv-\tau)^2)}{2\sigma}}\left(\bar{I}(\tau,\nu)-\mu_{\bar{I}}(\mathbf{p}\mid\sigma)\right)^{k}d\tau d\nu$$

### 2.5. 2D Examples of Multiscale Image Statistics

In the examples presented here, the term signal to noise ratio (SNR) will refer to the difference of the foreground intensity and the background intensity divided by the standard deviation of the additive spatially uncorrelated noise. Figure 8 shows a noisy computer generated image of a teardrop shape. The measured SNR per pixel within that image has been set to 4:1 on a raster resolution of 128 x 128 pixels.

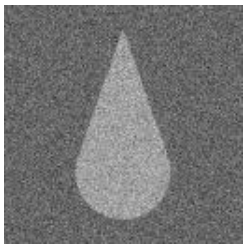

Figure 8. A 128 × 128 pixel Teardrop (SNR 4:1).

The images of Figure 9 are four local statistical measurements made of the teardrop using an aperture whose spatial aperture is 3 pixels wide. Figure 9a shows the local mean values. Figure 9b shows the measured local variances. Figures 9c and 9d show the local third and fourth moments respectively.

Figure 9 demonstrates aspects of multiscale statistical representations that are significant with respect to image processing tasks. The mean image is the input processed with a Gaussian filter. The variance image reflects edge strength and is analogous to the squared multiscale gradient magnitude of intensity. The third order local moment measurement has a locus of zero crossings along the boundary of the teardrop shape. This behavior is similar to the response of the Laplacian of the Gaussian on the same image.

## 3. Directional Statistics

The geometry of the image introduces important directional components that make directional sampling possible. Of interest then is a means of sampling in the direction in which the geometry of the image contributes the least bias to the statistical calculation, capturing the probability distribution of the noise rather than the structure of the image. In scalar-valued images this typically means sampling in the direction of the isophote.

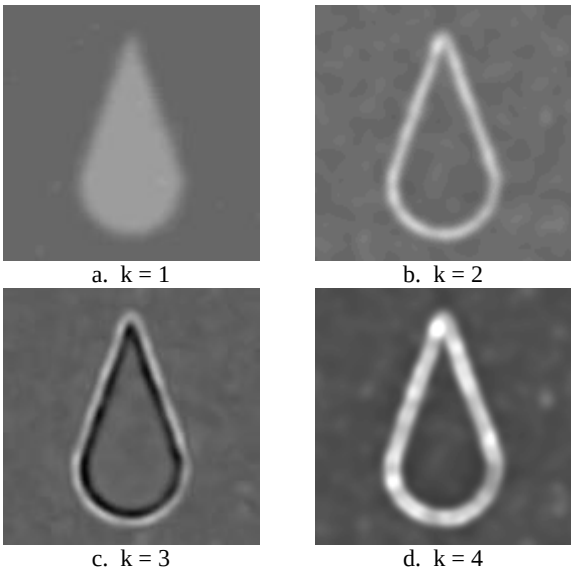

a. k = 1 b. k = 2 c. k = 3 d. k = 4

Figure 9. Local statistical measures (k = order) of the teardrop from Fig. 8 (a: local means, b: local variance, c and d: local moments of the 3rd and 4th order).

The direction of the tangent to the isophote is a sampling direction where the image can be considered to be locally mean-ergodic.

Minimizing the value of directional local statistics by repetitive application of directional statistical operators across all orientations is not desirable. An alternative is to establish a matrix that captures both local geometry and local image statistics. Once captured, this structured statistical operator can be analyzed for its eigenvalues and eigenvectors. Such an approach yields directional statistical analysis through a compact set of covariances.

### 3.1. Multiscale Directional Means

How can an image be sampled along a particular locus of minimal variation? Consider the local directional mean of an image to be a Gaussian weighted sample along a line. A multiscale directional mean $\mu_{\theta,I}(\mathbf{p}\mid\sigma)$ is defined as the integral along a line $l$ through the point $\mathbf{p} = [p_x, p_y]$, (that is $l$ is defined parametrically as $l_x(\rho) = \rho\cos\theta - p_x$ and $l_y(\rho) = \rho\sin\theta - p_y$) such that

$$\mu_{\theta,I}(\mathbf{p}\mid\sigma)=\int_{-\infty}^{\infty}\frac{1}{\sigma^2 2\pi}e^{\frac{-\rho^2}{2\sigma^2}}I(\rho\cos\theta-p_x,\rho\sin\theta-p_y)d\rho \quad (7)$$

Define $G_\theta(\sigma,\mathbf{p})$ to be a Gaussian distribution along a line $s$ through the origin (i.e., parametrically, $s$ is $s_x(\rho) = \rho\cos\theta$ and $s_y(\rho) = \rho\sin\theta$). $G_\theta(\sigma,\mathbf{p})$ can be expressed as

$$G_\theta(\sigma,\mathbf{p})=\begin{cases}\frac{1}{\sigma^2 2\pi}e^{\frac{-p_x^2-p_y^2}{2\sigma^2}} \text{ if } \frac{p_x^2}{p_x^2+p_y^2}=\cos^2\theta \text{ and } \frac{p_y^2}{p_x^2+p_y^2}=\sin^2\theta\\ \text{else } 0\end{cases} \quad (8)$$

(7) can be simplified using the following notation:

$$\mu_{\theta,I}(\mathbf{p} \mid \sigma) = G_\theta(\sigma, \mathbf{p}) \otimes I(\mathbf{p}) \tag{9}$$

### 3.2. Multiscale Directional Covariances

To generalize to second order directional moments, the linear directional means must be integrated over the sampling angle. Further, the directional variances must be weighted for sampling in either cardinal x direction or the cardinal y direction as provided by the original Cartesian coordinate axes. This results in the following sampled variance in the x-direction:

$$\begin{aligned} V_{xx} &= \mu^{(2)}_{x^2,I} \\ &= \int_0^\infty \int_{-\infty}^{\infty} \frac{1}{\sigma^2 2\pi} e^{\frac{-\rho^2}{2\sigma^2}} \left(\cos\theta\left(\left(I(\rho\cos\theta - p_x, \rho\sin\theta - p_x) - \mu_{\theta,I}(\mathbf{p} \mid \sigma)\right)\right)^2 d\rho d\theta \\ &= \frac{1}{\sigma\sqrt{2\pi}} \int_0^\pi \cos^2\theta\left(\left(G_\theta(\sigma,\mathbf{p}) \otimes (I(\mathbf{p}))^2\right) - \mu_{\theta,I}(\mathbf{p} \mid \sigma)\right)^2 d\theta \end{aligned} \tag{10}$$

Similarly, the variance in the y-direction is described as:

$$\begin{aligned} V_{yy} &= \mu^{(2)}_{y^2,I} \\ &= \frac{1}{\sigma\sqrt{2\pi}} \int_0^\pi \sin^2\theta\left(\left(G_\theta(\sigma,\mathbf{p}) \otimes (I(\mathbf{p}))^2\right) - \mu_{\theta,I}(\mathbf{p} \mid \sigma)\right)^2 d\theta \end{aligned} \tag{11}$$

For simplicity of notation, both the position parameter **p** and the scale parameter $\sigma$ have been dropped from the representation $V_{xx}$ and $V_{yy}$. The position and the scale or measurement aperture are always implicit in these measurements.

The covariance between intensity values measured in the x-direction and in the y-direction is described as:

$$\begin{aligned} V_{xy} &= \mu^{(2)}_{xy,I}(\mathbf{p} \mid \sigma) \\ &= \frac{1}{\sigma\sqrt{2\pi}} \int_0^\pi \sin\theta\cos\theta\left(\left(G_\theta(\sigma,\mathbf{p}) \otimes (I(\mathbf{p}))^2\right) - \mu_{\theta,I}(\mathbf{p} \mid \sigma)\right)^2 d\theta \end{aligned} \tag{12}$$

Taken together, these statistics describe a local feature space, centered about each pixel and normalized by the directional mean values. The resulting centered distribution has as its variance a $2 \times 2$ matrix or tensor:

$$\mathbf{C}_I(\mathbf{p} \mid \sigma) = \begin{bmatrix} V_{xx} & V_{xy} \\ V_{xy} & V_{yy} \end{bmatrix} \tag{13}$$

### 3.3. Eigenvalues and Eigenvectors

Since this matrix is symmetric and assuming that the rank of this matrix is not singular (i.e., the noise or variation in the image is not limited completely to a single directional bias), a matrix **D** can be found that this diagonalizes this covariance matrix. **D** can be shown to be a rotation.

$$\begin{aligned} \mathbf{D}\begin{bmatrix} V_{xx} & V_{xy} \\ V_{xy} & V_{yy} \end{bmatrix}\mathbf{D}^T &= \begin{bmatrix} V_{uu} & 0 \\ 0 & V_{vv} \end{bmatrix} \\ &= \begin{bmatrix} \cos\alpha & \sin\alpha \\ -\sin\alpha & \cos\alpha \end{bmatrix}\begin{bmatrix} V_{xx} & V_{xy} \\ V_{xy} & V_{yy} \end{bmatrix}\begin{bmatrix} \cos\alpha & \sin\alpha \\ -\sin\alpha & \cos\alpha \end{bmatrix} \end{aligned} \tag{14}$$

The eigenvalues $V_{uu}$ and $V_{vv}$ represent the variance of the directionally weighted intensity values in the direction of least and greatest variation respectively.

The direction $\alpha$ of the rotation matrix **D** indicates the direction of the two eigenvectors. Each eigenvector is oriented either tangentially along or perpendicular to the direction of least variance (e.g., tangent to object boundaries). The resulting eigenvectors of local image variance form a local coordinate frame or statistical gauge for geometrically invariant analysis methods.

Figure 10. shows a noisy 256 x 256 pixel image of a pair of curved objects. The measured SNR per pixel has been set to 4:1.

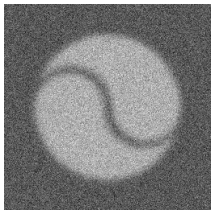

Figure 10. A $256 \times 256$ pixel figure (SNR 4:1)

The images of Figure 11 are the three local covariance measures statistical measurements made of the objects in the image using an aperture whose spatial aperture is 6 pixels. Figure 11a and Figure 11c show the weighted variance in the x and y-directions respectively. Figure 10b shows the related covariance between the sampled intensities when weighted in both x and y.

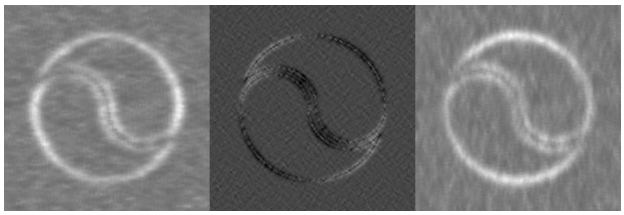

a. b. c.

Figure 11. Local statistical measures of Fig. 10 (Left a: $V_{xx}$, Center b: $V_{xy}$, and Right c. $V_{yy}$) ($\sigma = 6$)

Note the variations among the three images. In particular, compare Figure 11a with Figure 11c. Where the object boundary is perpendicular to the sampling direction, the response to the variance function is relatively higher. Where the sampling direction tangentially grazes the sampling direction, a relatively lower response is exhibited. With three covariance values at each pixel, a local covariance matrix is suggested. Diagonalizing this

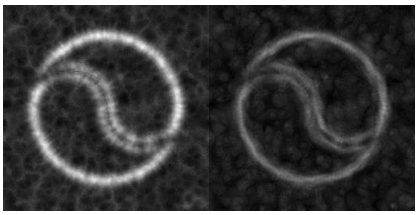

Figure 12. Eigenvalues of Fig. 11. (Left: $V_{uu}$, Right: $V_{vv}$,)

tensor image generates the eigenvalues in Figure 12. The eigenvalues show the weighted variance tangentially along or perpendicularly across the direction of greatest ergodicity, or constancy. In most cases this direction is either along or it is across the object boundaries. Figure 11 also shows the limitations imposed by discrete images and the subsequent tolerances imposed by the sampling theorem. In an ideal case, the eigenimage $V_{vv}$ should reflect only the variance of the background noise. However, the limited resolution of the available discrete methods introduces some isotropy into the sampling kernels yielding a ghost image. These values represent some contribution of the underlying image geometry to the generated statistical measurements.

### 3.4 Invariance w/rt linear functions of intensity.

The selection of the Gaussian function as the sampling kernel was motivated by a desire for the sampling filter to be invariant with respect to particular transformations of x. It may be desirable to analyze the sampled measurements of the array of $\bar{I}(x)$ values in dimensionless units (i.e., invariant with respect to certain transformations of $\bar{I}$). Dimensionless measurements may be obtained by normalizing the central moments with powers of the square root of $v_0$, the variance of the input noise (if known). That is:

Normalized k-th order moment: $$\gamma_{\bar{I}}^{(k)}(x \mid \sigma) = \frac{\mu_{\bar{I}}^{(k)}(x|\sigma)}{\left(\sqrt{v_0}\right)^k} \quad (15)$$

Without *a priori* knowledge of $v_0$, the normalization suggested in (15) can be implemented with $V_{vv}$ as the prior. This value is a multilocal measure of the local variance of image intensities where biases introduced by the underlying image geometry have been suppressed.

Normalized k-th order moment: $$\gamma_{\bar{I}}^{(k)}(\mathbf{p} \mid \sigma) = \frac{\mu_{\bar{I}}^{(k)}(\mathbf{p}|\sigma)}{\left(\sqrt{V_{vv}}\right)^k} \quad (16)$$

The results are dimensionless statistics that are invariant with respect to geometric operations such as translation and rotation, as well as linear functions of intensity (scaling, windowing, and leveling).

## 5. Applications and Future Work

Figure 13 shows zero-crossings of $\mu_{\bar{I}}^{(3)}(\mathbf{p} \mid \sigma)$ and its use as a boundary localizer. Interestingly, this operator closes boundaries in the presence of non-stationary changes in brightness and contrast. The contours extracted from the lower portions of the MRI of the head show this capability.

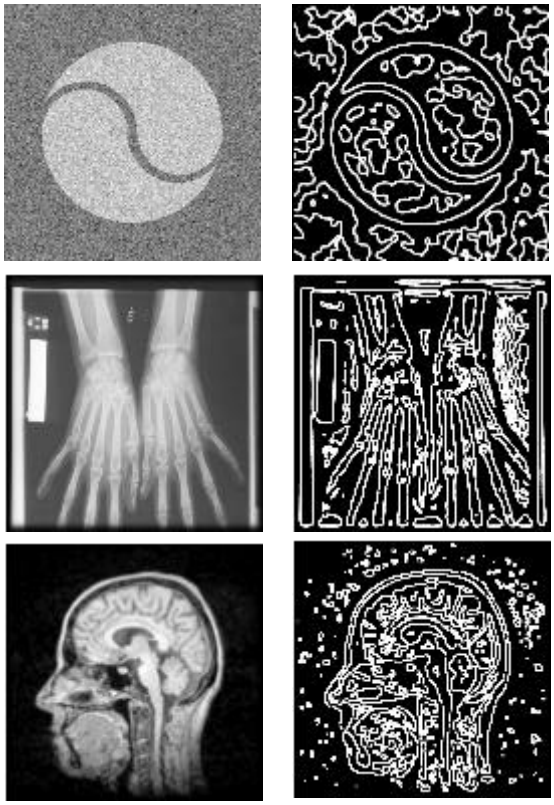

Figure 13. Test Images and zero crossings of $\mu_{\bar{I}}^{(3)}(\mathbf{p} \mid \sigma)$

Directional variances can also be combined into dimensionless metrics for texture analysis. A measure of anisotropy can be generated by mapping Lindeberg's anisotropy methods [18] from the partial derivatives of the *windowed second-moment matrix* to $V_{xx}$, $V_{yy}$, and $V_{xy}$. The resulting measure is shown in (17) and are graphically applied to a test image in Figure 14.

Anisotropy: $$\hat{Q} = \frac{\sqrt{(V_{xx}+V_{yy})^2 - 4(V_{xx}V_{yy} - V_{xy}^2)}}{V_{xx}+V_{yy}} \quad (17)$$

The future of this research will lie in the application of multiscale statistics to multivalued data. Research areas such as multimodal registration and multimodal segmentation require metrics that are normalized across multiple incommensurable values. Where Euclidean metrics are available, vector algebra may be employed. In the absence of such linearity, the calculus of statistics (and the use of multiscale image statistics) is appropriate.

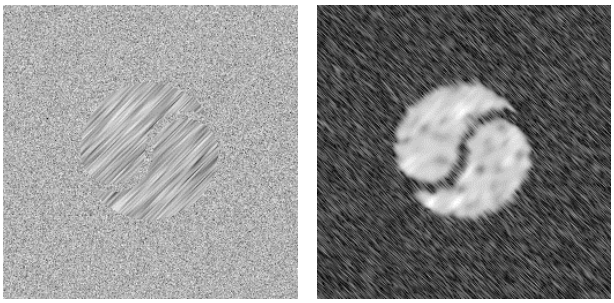

Figure 14. Segmentation of a textured test image with anisotropy metric $\hat{Q}$

## 6. Conclusion

Multiscale image statistics are a new means of capturing image geometry. Through scaled isotropic and directional statistical measurements, properties of local image structure can be extracted. Moreover, these measurements are invariant with respect to rotation, translation, and zoom, and they can be normalized to be invariant with respect to linear functions of intensity. These properties may support the analysis of images where vector valued methods are inappropriate (i.e., in statistical comparisons of multimodal datasets) and in modalities such as MR where there are non-stationary properties to image noise. Multiscale image statistics are new and important tools in image processing.

## References


[1] Babaud, J., A. Witkin, and R.O. Duda. 1986. Uniqueness of the Gaussian kernel for scale-space filtering. *IEEE Trans. Patt. Anal. Mach. Intell.* PAMI-8: 2-14.

[2] Chellappa, R., and A. Jain. 1993. *Markov Random Fields*. San Diego, CA: Academic Press.

[3] Cromartie, R. 1995. Structure-sensitive contrast enhancement: development and evaluation. Ph.D. diss., Univ. of North Carolina at Chapel Hill, Dept. of Computer Science.

[4] Demi, M. Contour Tracking by Enhancing Corners and Junctions. *Comp. Vision and Image Understanding*, 1996(63): 118-134.

[5] Dempster, A. P., N. M. Laird, and D. B. Rubin. 1977. Maximum likelihood from incomplete data via the EM algorithm. *J. Royal Statistical Society*. 1977(1): 1-38.

[6] Duda, R. O., and P. E. Hart. 1973. *Pattern Classification and Scene Analysis*. New York: John Wiley & Sons.

[7] Eberly, D. 1994. A differential geometric approach to anisotropic diffusion. in *Geometry-Driven Diffusion in Computer Vision,* ed. B.M. ter Haar Romeny, 371-392. Dordrecht, the Netherlands: Kluwer.

[8] Florack, L.M.J., B.M. ter Haar Romeny, J.J. Koenderink, and M.A. Viergever. 1994. General intensity transformations and differential invariants. *J. of Math. Imaging and Vis.* 4: 171-187.

[9] Florack, L.M.J., B.M. ter Haar Romeny, J.J. Koenderink, and M.A. Viergever. 1994. Images: regular tempered distributions. in *Shape in Picture*, 651-659. Berlin: Springer-Verlag.

[10] Geiger, D., and A. Yuille. 1991. A common framework for image segmentation. *Int. J. of Comp. Vis.* 6(3): 227-243.

[11] Geman S. and D. Geman. 1984. Stochastic relaxation, Gibbs distributions, and the Bayesian restoration of images. *IEEE Trans. Patt. Anal. Mach. Intell.* PAMI-6: 721-741.

[12] Gueziec, A. and N. Ayache. 1992. Smoothing and matching of 3-D space curves. *Visualization in Biomedical Computing 1992*, ed. Richard A. Robb. Proc. SPIE-1808: 259-273.

[13] Jain, A. K. 1989. *Fundamentals of Image Processing*. Englewood Cliffs, NJ: Prentice Hall.

[14] Koenderink, J.J. 1984. The structure of images. *Biol. Cybernet* 50: 363-370.

[15] Koenderink, J.J. 1990. *Solid shape*. Cambridge, MA: MIT press.

[16] Koenderink, J.J., and A.J. van Doorn. 1987. Representation of local geometry in the visual system. *Biol. Cybern.*, 55:367-375.

[17] Lee, J.S. 1983. Digital image smoothing and the sigma filter. *Comp. Vision, Graphics, and Image Processing.* CVGIP-24: 255-269.

[18] Lindeberg, T. 1994. *Scale Space Theory in Computer Vision*. Dordrecht, the Netherlands: Kluwer.

[19] Lindeberg, T. and B.M. ter Haar Romeny. 1994. Linear scale-space II: early visual operations. in *Geometry-Driven Diffusion in Computer Vision,* ed. B.M. ter Haar Romeny, 39-71. Dordrecht, the Netherlands: Kluwer.

[20] Perona, P. 1992. Steerable-scalable kernels for edge detection and junction analysis in *Proc. 2nd European Conf. On Comp. Vision*, Santa Margherita Ligure, Italy, May 1992, 3-18.

[21] Pizer, S.M., E.P. Amburn, J.D. Austin, R. Cromartie, A. Geselowitz, B.M. ter Haar Romeny, and J.B. Zimmerman. 1987. Adaptive histogram equalization and its variations. *Comp. Vision, Graphics, and Image Processing.* CVGIP-35: 355-368.

[22] ter Haar Romeny, B.M. and L.M.J. Florack. 1991. A multiscale geometric approach to human vision. in *Perception of Visual Information*, ed. B. Hendee and P. N. T. Wells, 73-114. Berlin: Springer-Verlag.

[23] ter Haar Romeny, B.M., L.M.J. Florack, A.H. Salden, and M.A. Viergever. 1993. Higher order differential structure in images. in *Proc. Int. Conf. Information Processing in Medical Imaging*, IPMI93, Flagstaff, AZ, USA, June 1993; Lecture Notes in Computer Science, 687, ed. H.H. Barrett, A.F. Gmitro, 77-93. Berlin: Springer-Verlag.

[24] Weickert, J. 1995. Multiscale texture enhancement. in *Proc. 6th Int. Conf. on Comp. Anal. of Images and Patt.* CAIP '95, Prague, Sep 1995. (Lecture Notes in Computer Science): Berlin: Springer-Verlag.

[25] Whitaker, R. T. and S. M. Pizer. 1993. A multi-scale approach to nonuniform diffusion, *CVGIP: Image Understanding*, 57(1);99-110, January 1993.

[26] Whitaker, R. T. 1993. Characterizing first and second order patches using geometry-limited diffusion. in *Information Processing in Medical Imaging* (Lecture Notes in Computer Science 687, H.H. Barrett and A.F. Gmitro, *eds.*): 149-167, Springer-Verlag, Berlin, 1993.

[27] Witkin, A. 1984. Scale-space filtering: a new approach to multi-scale description. in *Image Understanding 1984*, ed. S. Ullman, W. Richards, 79-95. Norwood, New Jersey: Ablex.